

# Genomic Signature for the Prognosis of Survival in Relation to the Tumor Microenvironment in Esophageal Adenocarcinoma

Yin Qin<sup>#</sup>, Minxian Tao<sup>#</sup>, Lili Song, Weihua Qian, Haijian Gao, Lianfang Liu, Yonghua Zhang<sup>\*\*</sup>, Yingying Pan<sup>\*\*</sup>

Department of Oncology, Zhangjiagang Traditional Chinese Medicine Hospital Affiliated to Nanjing University of Chinese Medicine, Zhangjiagang 215600, Jiangsu Province, China

<sup>#</sup>There authors contributed equally to this work

<sup>\*</sup>**Corresponding authors:** Yonghua Zhang, 241669122@qq.com; Yingying Pan, zjgzy037@njucm.edu.cn

**Copyright:** © 2022 Author(s). This is an open-access article distributed under the terms of the Creative Commons Attribution License (CC BY 4.0), permitting distribution and reproduction in any medium, provided the original work is cited.

**Abstract:** *Objective:* To establish a new genomic signature for the prognosis of survival in relation to the tumor microenvironment in esophageal adenocarcinoma. *Methods:* Data from The Cancer Genome Atlas (TCGA) were applied, and the stromal and immune scores of patients with esophageal adenocarcinoma (EAC) were generated through the ESTIMATE algorithm. Differentially expressed genes were obtained, and genes concerning immune prognosis were identified on the basis of these scores. Functional analysis showed that these genes were primarily involved in immunobiological processes. Additionally, CIBERSORT was used to analyze 22 subgroups of tumor-infiltrating immune cells in the tumor microenvironment. *Results:* The results of the genomic assessment shown on the Kaplan-Meier curve revealed that EAC patients with high-risk scores have the worst survival. The risk score is valid as an independent prognostic factor for the overall survival in EAC patients. The tumor microenvironment was systematically analyzed, and the immune-related prognostic biomarkers of EAC have been proposed. *Conclusion:* The expression of tumor-infiltrating immune cells and immune-related genes in EAC have been identified. Some previously overlooked genes may be used as additional biomarkers for EAC in the future.

**Keywords:** Esophageal adenocarcinoma; Genomic signature; Prognosis of survival; Tumor microenvironment

**Online publication:** March 23, 2022

## 1. Introduction

Esophageal cancer is one of the most common malignancies worldwide, and it has become the seventh most common cancer and the sixth leading cause of death globally <sup>[1]</sup>. Esophageal squamous cell carcinoma (ESCC) and esophageal adenocarcinoma (EAC) are the two main subtypes of esophageal cancer. Esophageal adenocarcinoma, which is commonly seen in many developed countries, mainly occurs in Barrett's esophagus. In terms of its histological progress, it usually develops from epithelial metaplasia to invasive carcinoma, usually located at the distal esophagus. It is closely related to gastro-esophageal reflux and obesity <sup>[2]</sup>. In spite of recent progress in its treatment and diagnosis, the 5-year survival rate for esophageal adenocarcinoma is still very poor <sup>[3]</sup>. Therefore, a further comprehending of cancer and exploring of treatment modes are essential to improve the prognosis of EAC patients.

In recent years, people have gradually realized the function of tumor microenvironment (TME) in tumor biology. Tumor microenvironment refers to the cellular environment in which tumors are generated. It includes immune cells, endothelial cells, mesenchymal cells, inflammation agents, and extracellular matrix (ECM) [4,5]. The cells and molecules in the tumor microenvironment are dynamically changing, indicating the nature of tumor growth and mutually promoting immune absconding, tumor breeding, and metastasis [6]. In the tumor microenvironment, immune cells and stromal cells are the two main non-neoplastic components that are considered to be the focus of prognostic assessment and tumor diagnosis. Therefore, comprehending the molecular structure and usage of the tumor microenvironment is the key to control tumor evolution and immune response. The expression of unique molecular biomarkers in immune cells and stromal cells has been determined, and a tumor microenvironment prediction algorithm based on immune/stromal/ESTIMATE scores has been established [7]. On the basis of the ESTIMATE algorithm, researchers have evaluated the prognosis of many tumors and explored gene changes [8-10]. However, the value of immune/stromal scores for EAC has not been investigated in detail.

In this study, based on the exploration of the tumor microenvironment, immune-related prognostic biomarkers were traced in EAC, using both EAC cohorts of The Cancer Genome Atlas (TCGA) database and ESTIMATE algorithm.

## **2. Materials and methods**

### **2.1. Data acquisition**

The gene expression profiles of patients with EAC were downloaded along with clinical data on gender, age, tissue type, TNM staging, survival, and outcome from the TCGA website (<https://portal.gdc.cancer.gov/>). The selected standards were: (1) patients with EAC; (2) available overall survival (OS) data; (3) available raw count or normalized gene expression data. The downloaded data were used to calculate the stromal and immune scores via the ESTIMATE database (<https://bioinformatics.mdanderson.org/estimate/>).

### **2.2. Identification of differentially expressed genes (DEGs)**

The TCGA cohort was stratified according to the intermediate values of the stromal/immune scores. The low- and high-risk groups of DEGs were obtained by applying the “limma” package [11]. The cut-off values for the screening of DEGs were fold change of  $> 2$ ,  $P < 0.05$ , and false discovery rate (FDR) of  $< 0.05$ .

### **2.3. Heatmaps and Venn diagrams**

The “Heatmap” R package was used to conduct heatmaps, and the “VennDiagram” package was used to generate Venn diagrams.

### **2.4. Bioinformatics analysis**

The GO enrichment analysis of DEGs was generated by applying the “clusterProfiler” package. Meanwhile, KEGG (Kyoto Encyclopedia of Genes and Genomes) pathway enrichment analysis was obtained by the package. The PPI network was carried out through the Metascape website (<http://metascape.org>) [12] with default parameters.

### **2.5. Construction of the immune-related risk signatures**

The endpoint was considered as the overall survival. The model was used to perform an overall survival analysis for verification. First, a preliminary screening of genes was conducted through univariate Cox regression. Next, in order to select the prognostic genes, the least absolute shrinkage and selection operator (LASSO) Cox regression model was used [13]. The “survival” and “glmnet” R packages were used to

analyze and obtain the model. Based on the results from LASSO Cox regression, immune-related risk signatures were established for the TCGA cohort. The risk score of each patient was calculated by taking advantage of both the gene expression levels and LASSO-Cox regression coefficients. The patients were divided into low- and high-risk groups on the basis of the median risk score, and the survival rates between the two groups were estimated based on a combination of Kaplan-Meier curve and log-rank analysis. The “timeROC” package was used to perform the time-dependent receiver operating characteristic (ROC) curve of the risk scores to identify the prognostic precision of risk scores. Finally, the independent prognostic values of risk scores and other clinical features were explored using univariate and multivariable Cox analysis.

## 2.6. Survival analysis

Kaplan-Meier curves were applied to determine genes that could independently predict the OS of EAC patients. Kaplan-Meier curves were generated using the “survival” R package.

## 2.7. Evaluation of immune cell infiltration

CIBERSORT algorithm was used to calculate tumor-infiltrating immune cells <sup>[14]</sup>. CIBERSORT (<https://cibersortx.stanford.edu/index.php>) is a web tool, which has a gene expression signature matrix of 547 marker genes, applied to characterize the abundance of 22 immune cell types. The 22 immune cell subtypes include memory B cells, naive B cells, seven types of T cells, resting NK cells, activated NK cells, plasma cells, monocytes, M0-M2 macrophages, eosinophils, neutrophils, resting dendritic cells, activated dendritic cells, resting mast cells, and activated mast cells. In this study, CIBERSORT was used with a signature matrix at 1000 permutations to reckon the numbers and ranges of immune cell types in the case of transcriptome data as well as the distinctions in immune cell type composition among various groups. The results of the estimation were visualized with “barplot” and “vioplot” R packages.

## 3. Results

### 3.1. Differentially expressed gene analysis based on stromal/immune scores via the ESTIMATE algorithm

In order to explore the relationships between the gene expression profiles and the stromal/immune scores, the RNA-sequencing data of the 79 EAC cases were downloaded from the TCGA database for analysis. Among these patients, there were 11 (13.92%) female patients and 68 (86.08%) male patients. The clinical characteristics of the patients are shown in **Table 1**. Based on the ESTIMATE algorithm, these patients were divided into high-score and low-score groups according to the median values of the stromal and immune scores. The heatmaps in **Figure 1A** and **1B** revealed significant transcriptome data of the samples between the high and low stromal/immune score groups.

In addition, the Venn diagrams of differentially expressed genes (DEGs) were drawn (**Figure 1C**, **1D**, and **1E**). According to the aforementioned threshold (fold change > 2,  $P < 0.05$ , and false discovery rate < 0.05), 1,516 DEGs were obtained between high and low stromal groups and 988 DEGs were obtained between high and low immune score groups. Additionally, 835 genes were upregulated, and 1 gene was downregulated simultaneously between the stromal and immune score groups.

**Table1.** Clinical characteristics of patients with EAC in the TCGA database

<b>Variables</b>	<b>Cases, N (%)</b>
Age at diagnosis	
≤ 60	30 (37.97%)
>60	49 (62.03%)
Gender	
Female	11 (13.92%)
Male	68 (86.08%)
Pathological stage	
I	9 (11.39%)
II	22 (27.85%)
III	27 (34.18%)
IV	5 (6.33%)
NA	16 (20.25%)
TNM-T	
T0	1 (1.27%)
T1	19 (24.05%)
T2	10 (12.66%)
T3	36 (45.57%)
T4	1 (1.27%)
NA	12 (15.19%)
TNM-N	
N0	20 (25.32%)
N1	37 (46.84%)
N2	4 (5.06%)
N3	5 (6.33%)
NX	1 (1.27%)
NA	12 (15.19%)
TNM-M	
M0	51 (64.56%)
M1	5 (6.33%)
MX	9 (11.39%)
NA	14 (17.72%)

Note: NA, non-applicable

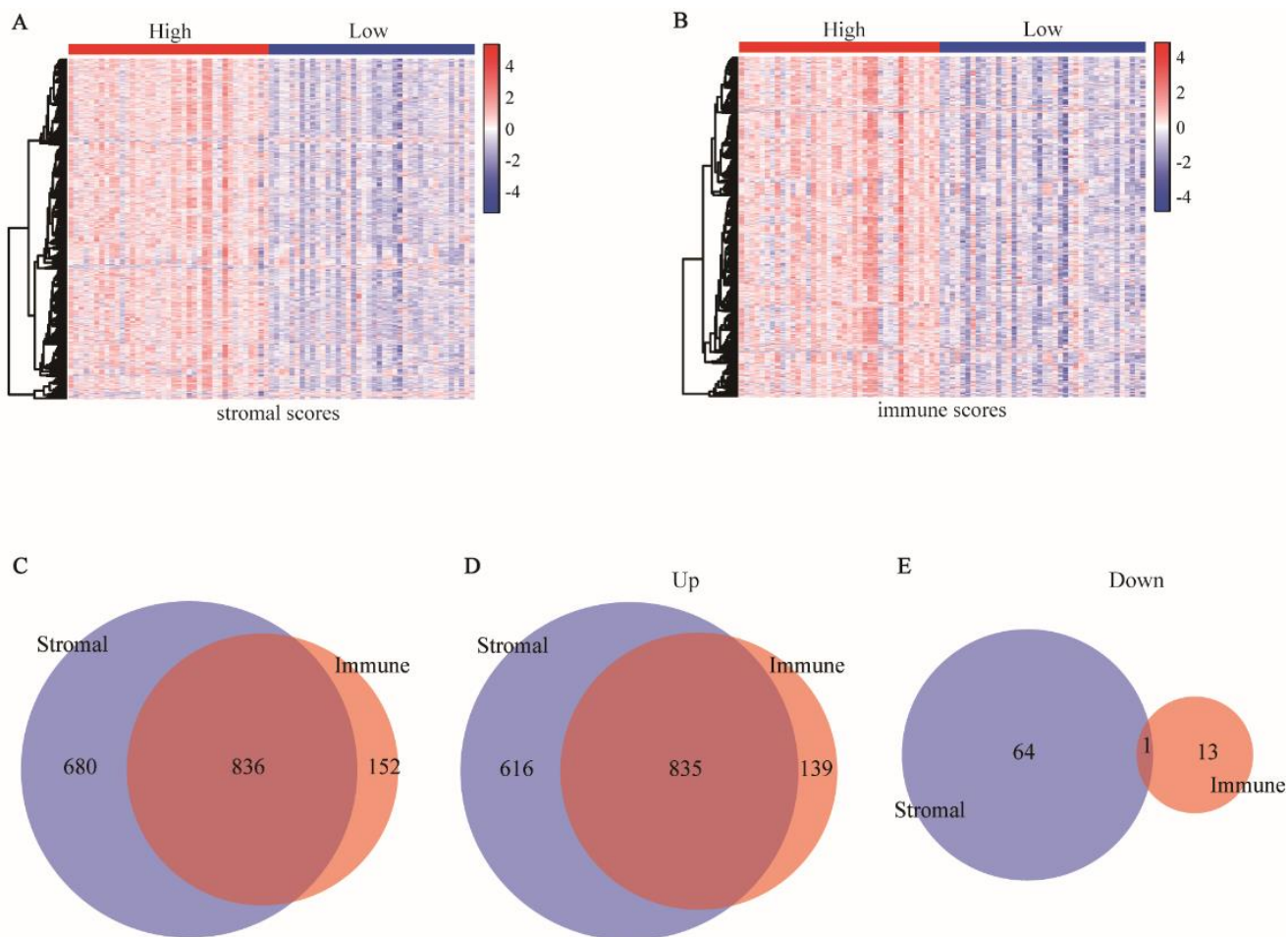


**Figure 1.** Stromal and immune scores of gene expression profiles in EAC; (A)(B) Heatmaps displaying distinct expressed genes according to stromal and immune scores; red marker reflects higher expression genes and blue marker reflects lower expression genes; (C)(D)(E) Venn diagrams of simultaneously differentially expressed genes drawn according to stromal and immune scores

### 3.2. GO and KEGG enrichment analyses for DEGs

Gene Ontology (GO) and Kyoto Encyclopedia of Genes and Genomes (KEGG) analyses of co-DEGs using the “clusterProfiler” package were carried out to assess the differentially expressed genes on the tumor-infiltrating immune cells. The heatmap in **Figure 2A** exhibited 30 enriched terms of GO among the DEGs on the basis of biological process (BP), cellular component (CC), and molecular function (MF) for EAC cohorts; the heatmap in **Figure 2B** exhibited 15 enriched pathways of KEGG among the DEGs. Majority of these terms or pathways are related to cell activation and cell adhesion molecules (CAMs). Consistent with the GO and KEGG analyses, protein-protein interaction (PPI) networks were colored through different cluster ID (**Figure 2C**) and *P*-value (**Figure 2D**), which were generated using Metascape. As most networks from the DEGs are associated with immune response, the results indicated that the differentially expressed genes obtained according to stromal and immune scores were significant.

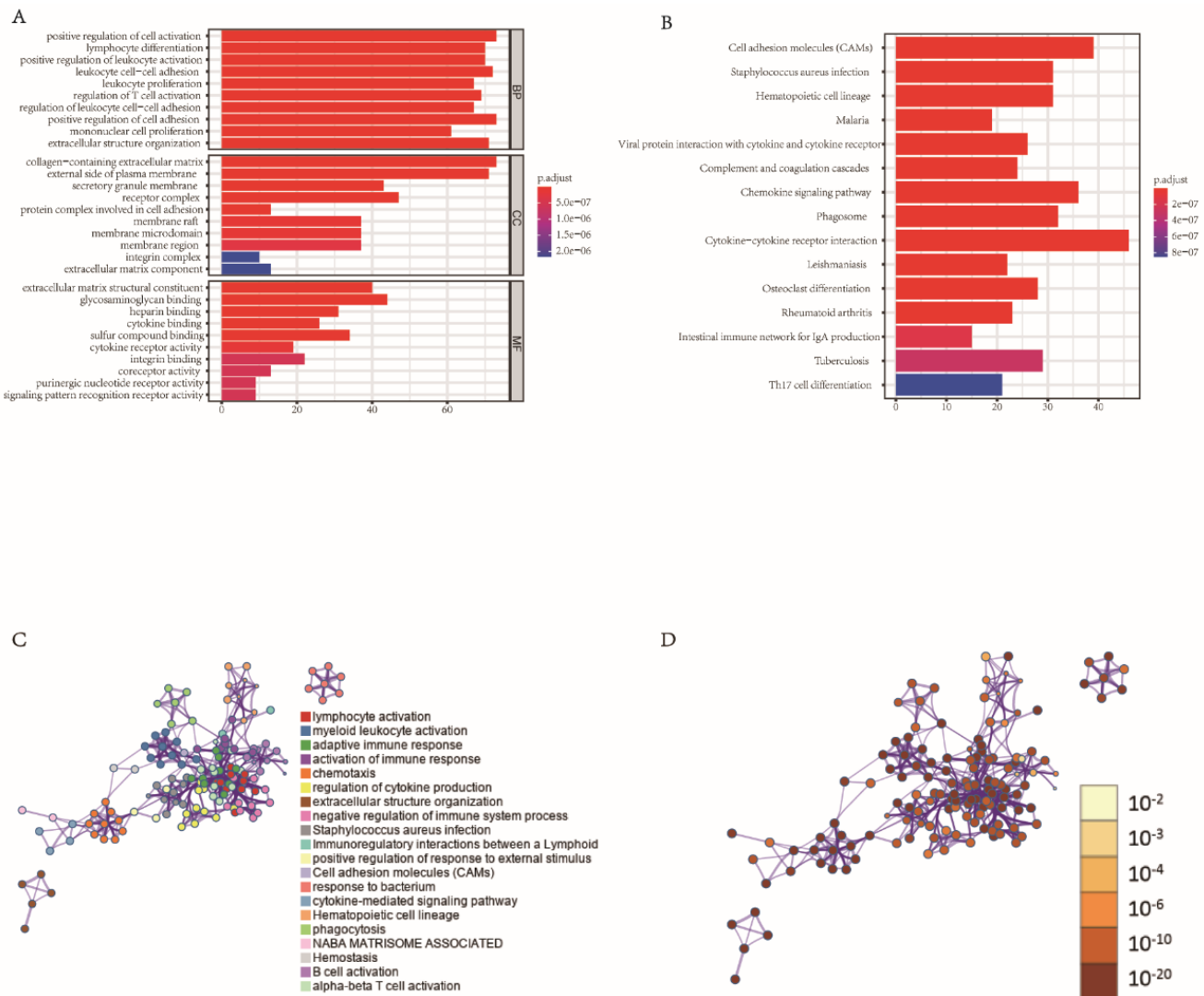


**Figure 2.** GO and KEGG enrichment analyses of DEGs; **(A)** GO analysis of DEGs, including biological process (BP), cellular component (CC), and molecular function (MF); **(B)** KEGG analysis of DEGs; **(C)** Protein-protein networks colored by different cluster ID; **(D)** Protein-protein networks colored by *P*-value

### 3.3. Establishment of genomic signature for the prognostic survival of EAC patients

According to the 836 DEGs in the stromal and immune score groups of the EAC patients, a preliminary screening was performed using Cox univariate regression to eliminate over confounding gene interference and obtain those genes that have the greatest effect on prognosis. In order to prevent the exclusion of significant genes, 29 genes with  $P < 0.1$  were screened and switched to LASSO regression. The LASSO coefficient profiles of the 29 genes (**Figure 3A**) were presented, and the results from a 10-fold cross-validation were provided to determine the best value of the penalty parameter  $\lambda$  (**Figure 3B**).

The forest map revealed the relationship between each gene and overall survival (**Figure 3C**). Ultimately, a genomic signature with seven genes (RASGRP2, TNXB, ZBTB16, MASP1, TLR6, TNFRSF13C, and CXCL10) was selected to construct a prediction model for patients with EAC according to the gene expression levels and their regression coefficients:

$$\text{Risk score} = (0.12264 \times \text{expression level of RASGRP2}) + (-0.09632 \times \text{expression level of TNXB}) + (-0.0091 \times \text{expression level of ZBTB16}) + (-0.12716 \times \text{expression level of MASP1}) + (-0.1131 \times \text{expression level of TLR6}) + (-0.18604 \times \text{expression level of TNFRSF13C}) + (0.06844 \times \text{expression level of CXCL10})$$

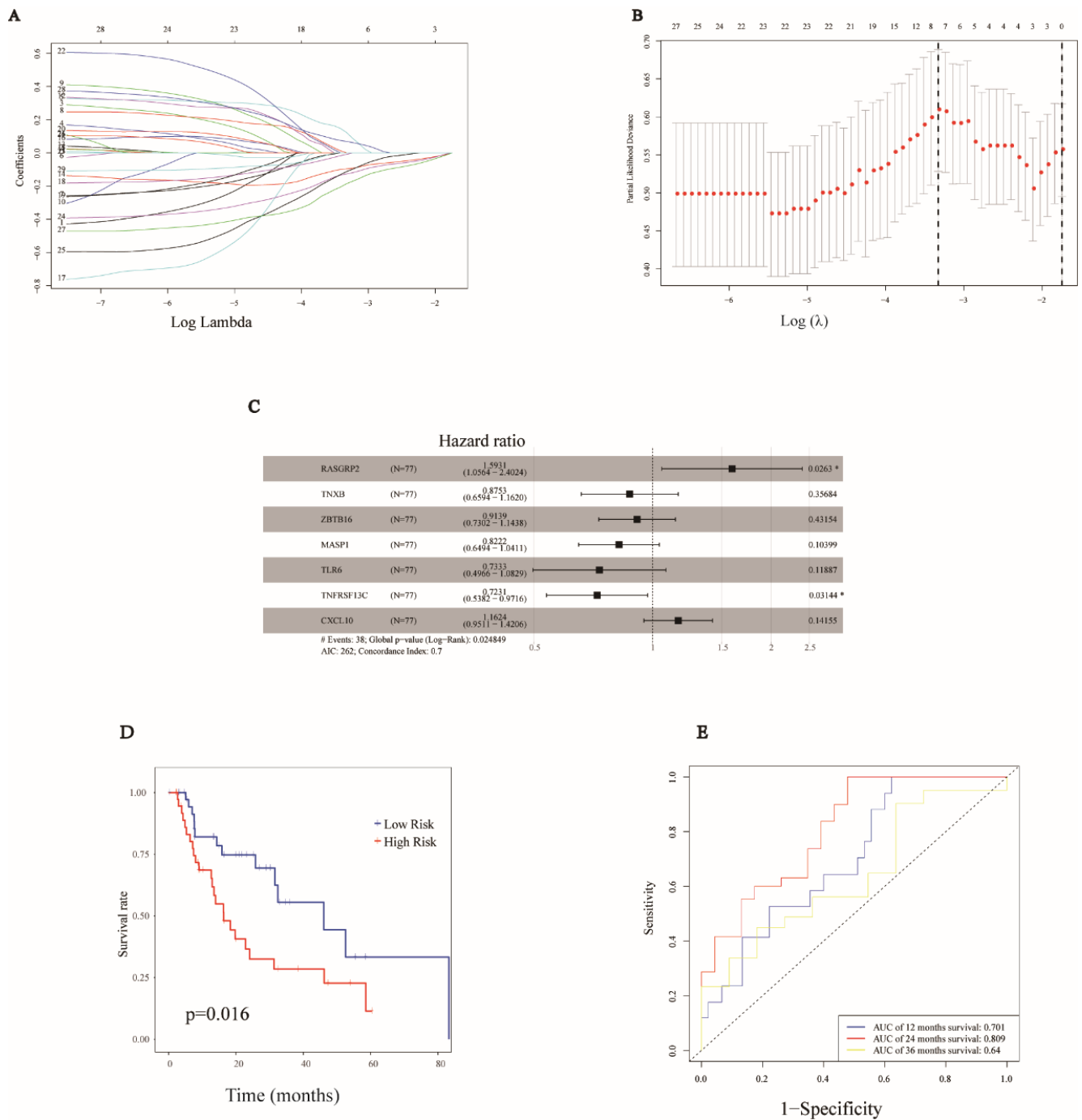


**Figure 3.** Establishment of genomic signature for the prognostic survival of EAC patients; **(A)** LASSO coefficient profiles of 29 genes with  $P < 0.1$ ; **(B)** The optimal values of the penalty parameter  $\lambda$  determined by 10-fold cross-validation; **(C)** Association of genes with overall survival; **(D)** Kaplan-Meier curves in EAC patients; **(E)** ROC curves of 1-year, 2-year, and 3-year OS of EAC patients.

The median risk score was set as the cut-off value to divide EAC patients into low-risk and high-risk groups. The Kaplan-Meier curve revealed that low-risk patients had better survival rates ( $P = 0.016$ ) (**Figure 3D**). Meanwhile, multivariate analysis also showed that the genomic signature with seven genes could independently predict the survival of EAC patients ( $P = 0.005$ , **Table 2**). The AUCs of time-dependent ROC for 1-year, 2-year, and 3-year OS of the EAC dataset were 0.701, 0.809, and 0.64, respectively (**Figure 3E**). Therefore, the ROC curve confirmed the favorable effect of risk score in exerting prognostic value for esophageal adenocarcinoma.

**Table 2.** Univariate and multivariate analyses of prognostic factors in EAC patients

Variables	EAC cohort			
	Univariate analysis		Multivariate analysis	
	HR (95%CI)	<i>P</i>	HR (95%CI)	<i>P</i>
Age	0.98 (0.95-1)	0.075		
Gender	0.91 (0.32-2.6)	0.860		
Race	0.73 (0.54-0.98)	0.039	0.55 (0.31-0.97)	0.038
Tumor stage	2.5 (1.4-4.3)	< 0.001	3.16 (1.24-8.04)	0.016
Grade	2 (0.95-4.3)	0.070		
Risk score	4.8 (2-12)	< 0.001	16.83(2.35-120.36)	0.005

### 3.4. Survival analysis of simultaneously differentially expressed genes

In order to investigate the regulatory mechanism of EAC prognosis, Kaplan-Meier curves were generated using gene expression levels and overall survival. The study illustrated that MASP1, TNFRSF13C, and ZBTB16 were statistically significantly associated with the overall survival of EAC (**Figure 4A, 4B, and 4C**).

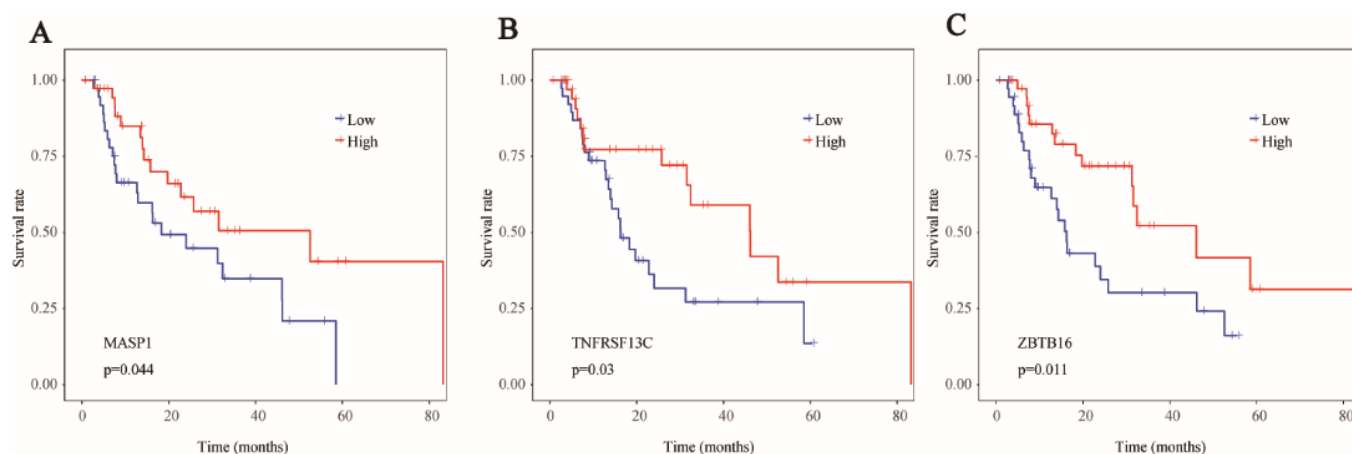


**Figure 4.** Correlations of immune-related DEGs with overall survival of EAC cohort; (A)(B)(C) Prognosis-related DEGs in EAC; the Kaplan-Meier survival curves were drawn based on immune-related DEGs selected from high (red line) and low (blue line) gene expression groups; log-rank test evaluated the differences with  $P < 0.05$ .

### 3.5. Immune microenvironment in EAC

In order to completely comprehend the immune and stromal signature, the proportions of immune cells in tumor tissues were determined in comparison with those in adjacent normal tissues (i.e., 79 tumor samples with EAC and 10 normal samples). As shown in **Figure 5A**, the results of CIBERSORT revealed that the infiltration levels of activated memory  $CD_4^+$  T cells ( $P = 0.046$ ) and resting NK cells ( $P = 0.041$ ) were significantly higher in tumor tissues compared with normal tissues in patients with EAC; however,  $CD_8$  T cells ( $P = 0.028$ ), activated NK cells ( $P = 0.001$ ), and eosinophils ( $P < 0.001$ ) were higher in normal tissues. Moreover, the infiltration levels of naive B cells ( $P = 0.015$ ) were relatively lower in the high-risk group compared with the low-risk group (**Figure 5B**) in EAC cohorts.



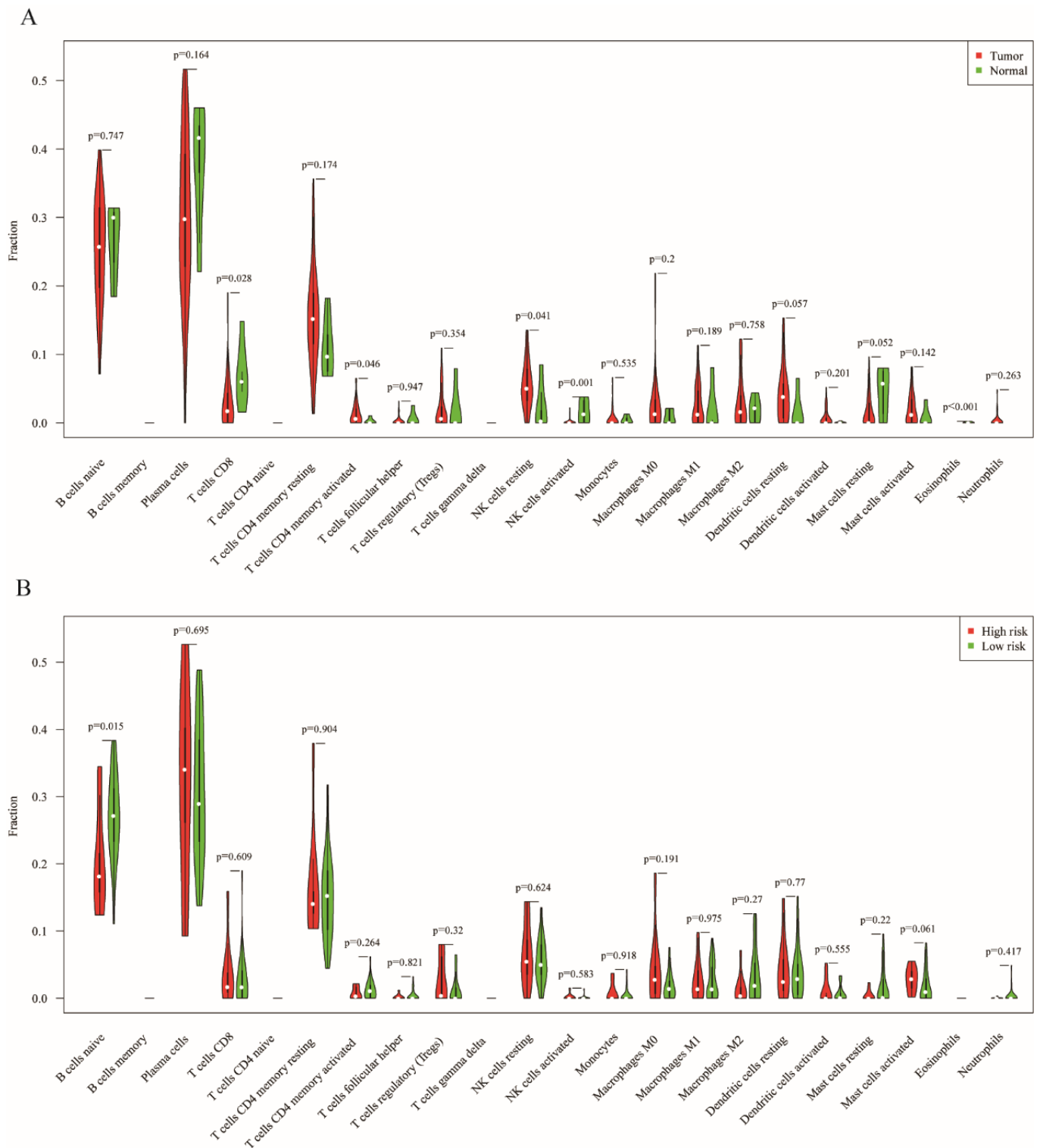


**Figure 5.** Infiltrated immune cells in EAC cohort using the CIBERSORT algorithm; **(A)** Differential abundance of immune infiltration between tumor tissues and normal tissues in EAC; **(B)** Differential abundance of immune infiltration between high-risk groups and low-risk groups;  $P < 0.05$  is considered statistically significant.

#### 4. Discussion

In recent years, with the improvement of treatment methods, such as radiotherapy, chemotherapy, targeted therapy, and immunotherapy, the survival of patients with esophageal cancer has improved, but the prognosis is still poor. The lack of effective prognostic biomarkers to guide the treatment of cancer is the

essential reason for the poor prognosis. A number of research studies have indicated that tumor microenvironment is a potential target for tumor therapy. First of all, cells in the tumor microenvironment, which have fewer mutations, selective pressure, and lower opportunity of developing drug resistance, are genetically more stable than cancer cells. Furthermore, owing to the lack of ability to depend on genetic mutations to conduct movement, the tumorigenicity of cells in the tumor microenvironment mainly depends on the factors in their environment. Consequently, they can be affected by the interaction of destructive environmental and other factors to drive functional changes during tumorigenesis<sup>[15]</sup>. Therefore, TCGA was used for bioinformatics analysis to identify immune-related genes in the tumor microenvironment that could predict the prognosis of EAC patients.

In order to distinguish immune-related genes and comprehend the tumor microenvironment of EAC, stromal and immune scores were obtained using the ESTIMATE algorithm. By comparing the transcriptional expression profiles of 79 EAC patients with high and low stromal/immune scores, 835 upregulated DEGs and 1 downregulated DEG were obtained. It appeared that these common DEGs are involved in crucial immune response processes, including cell activation and cell adhesion molecules (CAMs), indicating that dynamic immune microenvironments and responses in EAC might explain tumorigenesis and advancement with meaningful potential influences on the prognosis of patients.

A new method of stratifying patients according to the different immune microenvironment scores was used to identify the DEGs. The intersected genes concerning prognosis-related genes selected from the univariate Cox regression method were subjected to LASSO regression with a 10-fold cross-validation to screen out seven novel DEGs (RASGRP2, TNXB, ZBTB16, MASP1, TLR6, TNFRSF13C, and CXCL10) in EAC. In the EAC cohort, a prognostic predictive model was established based on seven genes. RASGRP2 and CXCL10 are risk immune-related genes, while TNXB, ZBTB16, MASP1, TLR6, and TNFRSF13C are protective genes. The predictive model separated the patients into high- and low-risk groups according to their median risk scores. Accordingly, the risk scores were independently associated with the prognosis of EAC patients, and the outcomes were better in the low-risk group rather than the high-risk group ( $P < 0.05$ ).

The Kaplan-Meier survival curves revealed that MASP1, TNFRSF13C, and ZBTB16 were independently associated with prognosis.

Mannose-binding lectin (MBL) is a component in the serum that activates complement through a new way to participate in innate immunity<sup>[16]</sup>. Human MBL forms complexes with serine proteases termed MASP (MBL-associated serine protease). In the activation of the lectin channel, MBL-associated serine proteases (MASP-1, MASP-2, MASP-3, MASP-4, and MASP-19) are key elements. The serum grades of these factors have been related to low survival of several cancer types, including colorectal cancer, ovarian cancer, and cervical cancer<sup>[17-19]</sup>.

BAFF receptor (BAFF-R/BR3/TNFRSF13C) is regarded as a presently discovered molecule that binds BLyS, a protein which is a part of the tumor necrosis factor (TNF) family, and has an impact on the survival and maturation of B cells<sup>[20]</sup>. A number of B-cell malignancies, for instance diffuse large B-cell lymphoma (DLBCL), express BAFF-R, and its activation promotes proliferation and survival of DLBCL cells<sup>[21-24]</sup>. ZBTB16 was first discovered in a patient with acute promyelocytic leukemia. It is an inhibitory zinc-finger transcription factor, which is a part of POZ (poxvirus and zinc finger) – Krüppel family<sup>[25,26]</sup>. ZBTB16 is involved in many different signal pathways of hematopoietic cells and solid tumors, such as cell cycle, differentiation, and programmed cell death<sup>[25,27]</sup>.

In view of the activity of novel genes in the process of tumorigenesis and the marked association with the prognosis of EAC patients, they may possess the performance of new tumor biomarkers if their specific roles in EAC are known in detailed through extensive investigations.

Tumor-infiltrating immune cells have a great impact on the tumor microenvironment. When using immune checkpoint inhibitors, tumor infiltrating immune cells should be considered, because the effectiveness of immune checkpoint blockade requires immune cell infiltration [28,29]. The abundance of 22 immune cell subsets was calculated using the CIBERSORT algorithm, and the effect of tumor-infiltrating immune cells in esophageal carcinoma was illustrated. In this present study, the immune cell subsets in tumor tissues of EAC were significantly different from those in normal tissues; in EAC patients, the activated memory CD4<sup>+</sup> T cells, CD8 T cells, resting NK cells, activated NK cells, and eosinophils were significantly different in tumor tissues compared with those in normal tissues; in addition, the infiltration levels of naive B cells were significantly higher in the low-risk group. The results revealed that these immune cells may play an important role in the tumor microenvironment of EAC. A meta-analysis concluded that extensive tumor-infiltrating lymphocytes (TILs) are excellent prognostic indicators for the overall survival in patients with esophageal carcinoma (ESCA) [30]. It was found that activated memory CD4<sup>+</sup> T cells in tumor-infiltrating lymphocytes (TILs) widely infiltrated tumor tissues; however, CD8 T cells were universally discovered in normal tissues of EAC patients. The degree of tumor-infiltrating lymphocytes, especially activated CD8<sup>+</sup> T cells in melanoma, was found to be positively correlated with a better prognosis [31]. However, in another study involving 130 patients with esophageal adenocarcinoma, CD8<sup>+</sup> lymphocyte was found to have no associated with survival [32]. These results may suggest that immune cells have dual effects (host protection and tumor promotion) in different types of tumors [33,34]. Notably, it has been suggested that CD4<sup>+</sup> T cells are correlated with good prognosis in patients with esophageal carcinoma [35]; however, it was found that CD4<sup>+</sup> TILs are not associated with the survival of ESCA patients [30]. In the findings of this study, activated memory CD4<sup>+</sup> T cells were found to be higher in tumor tissues than in normal tissues of the EAC cohort. These controversial results may be due to tissue microenvironmental factors, which may change the phenotype and function of T cells early during esophageal disease progression and may function as targets for immune intervention [36]. Further research associated with the impact of immune-infiltrating cell balance on clinical outcomes is necessary.

In recent years, it has been recognized that B cells play a very complex role in the tumor microenvironment, as some subsets of B cells may have immunomodulatory functions [37]. In this research, naive B cells were found to be associated with a low-risk score for esophageal adenocarcinoma, and it was hypothesized that they may be associated with good prognosis in patients with esophageal adenocarcinoma. However, the relationship between the subsets of B cells and the prognosis of patients with esophageal adenocarcinoma has not been defined.

Currently, the number of studies on the prognostic value of infiltrated NK cells in esophageal adenocarcinoma are very limited. In the future, more relevant studies are needed to further clarify the relationship between immune cells, such as NK, and the prognosis of esophageal adenocarcinoma.

There are several limitations in this study. First, this study was a retrospective study, in which the data of gene expression as well as clinical information were downloaded from the TCGA database; hence, selection and recall biases are inevitable. Second, the values of prognosis in EAC patients could not be fully elucidated due to the lack of comprehensive chemoradiotherapy in this study. Moreover, the present study did not rely on other available databases for external validation; thus, further investigations are required to study the mechanisms by which the immune-related prognostic genes regulate the initiation and progression of EAC.

In conclusion, the expression of tumor-infiltrating immune cells and immune-related genes in EAC have been identified. Some previously overlooked genes may be used as additional biomarkers for EAC. Further *in vivo* and *in vitro* studies are required to explore the mechanisms through which the immune cells and genes are involved in EAC progression to promote advancement in EAC treatment.

## Acknowledgments

The authors would like to express their sincere thanks to the US National Cancer Institute for sharing their TCGA data.

## Funding

College-Level Youth Fund Project (Project Number: ZZYQ2012).

## Disclosure statement

The authors declare no conflict of interest.

## Author contributions

YP and YZ designed and edited this study; LS, WQ, HG, and LL searched the databases and collected the data; YQ and MT analyzed the data and wrote the manuscript. All authors read and approved the final manuscript.

## References

- [1] Bray F, Ferlay J, Soerjomataram I, et al., 2018, Global cancer Statistics 2018: GLOBOCAN Estimates of Incidence and Mortality Worldwide for 36 Cancers in 185 Countries. *CA: A Cancer Journal for Clinicians*, 68(6): 394-424.
- [2] Ho ALK, Smyth EC, 2020, A Global Perspective on Oesophageal Cancer: Two Diseases in One. *The Lancet Gastroenterology & Hepatology*, 5(6): 521-522.
- [3] Short MW, Burgers KG, Fry VT, 2017, Esophageal Cancer. *American Family Physician*, 95(1): 22.
- [4] Hanahan D, Weinberg RA, 2000, The Hallmarks of Cancer, 100(1): 0-70.
- [5] Hanahan D, Coussens LM, 2012, Accessories to the Crime: Functions of Cells Recruited to the Tumor Microenvironment. *Cancer Cell*, 21(3): 309-322.
- [6] Jiang X, Wang J, Deng X, et al., 2019, Role of the Tumor Microenvironment in PD-L1/PD-1-Mediated Tumor Immune Escape. *Molecular Cancer*, 18(1): 1-17.
- [7] Yoshihara K, Shahmoradgoli M, Martinez E, et al., 2013, Inferring tumour Purity and Stromal and Immune Cell Admixture from Expression Data. *Nat Commun*, 4: 2612.
- [8] Jia D, Li S, Li D, et al., 2018, Mining TCGA Database for Genes of Prognostic Value in Glioblastoma Microenvironment. *Aging (Albany NY)*, 10(4): 592.
- [9] Shah N, Wang P, Wongvipat J, et al., 2017, Regulation of the Glucocorticoid Receptor Via a BET-Dependent Enhancer Drives Antiandrogen Resistance in Prostate Cancer. *Elife*, 6: e27861.
- [10] Alonso MH, Ausso S, Lopez-Doriga A, et al., 2017, Comprehensive Analysis of Copy Number Aberrations in Microsatellite Stable Colon Cancer in View of Stromal Component. *British Journal of Cancer*, 117(3): 421-431.
- [11] Ritchie ME, Phipson B, Wu D, et al., 2015, Limma Powers Differential Expression Analyses for RNA-Sequencing and Microarray Studies. *Nucleic Acids Res*, 43(7): e47.
- [12] Zhou Y, Zhou B, Pache L, et al., 2019, Metascape Provides a Biologist-Oriented Resource for the Analysis of Systems-Level Datasets. *Nat Commun*, 10(1): 1523.

- [13] Shahraki HR, Salehi A, Zare N, 2015, Survival Prognostic Factors of Male Breast Cancer in Southern Iran: a LASSO-Cox Regression Approach. *Asian Pac J Cancer Prev*, 16(15): 6773-6777.
- [14] Newman AM, Liu CL, Green MR, et al., 2015, Robust Enumeration of Cell Subsets from Tissue Expression Profiles. *Nature Methods*, 12(5): 453-457.
- [15] Lin EW, Karakasheva TA, Hicks PD, et al., 2016, The Tumor Microenvironment in Esophageal Cancer. *Oncogene*, 35(41): 5337-5349.
- [16] Matsushita M, Endo Y, Fujita T, 1998, MASP1 (MBL-Associated Serine Protease 1). *Immunobiology*, 199(2): 340-347.
- [17] Swierzko AS, Szala A, Sawicki S, et al., 2014, Mannose-Binding Lectin (MBL) and MBL-associated serine protease-2 (MASP-2) in women with malignant and benign ovarian tumours. *Cancer Immunol Immunother*, 2014. 63(11): p. 1129-40.
- [18] Ytting H, Christensen IJ, Steffensen R, et al., 2011, Mannan-Binding Lectin (MBL) and MBL-Associated Serine Protease 2 (MASP-2) Genotypes in Colorectal Cancer. *Scand J Immunol*, 73(2): 122-127.
- [19] Maestri CA, Nisihara R, Mendes HW, et al., 2018, MASP-1 and MASP-2 Serum Levels Are Associated with Worse Prognostic in Cervical Cancer Progression. *Front Immunol*, 9: 2742.
- [20] Losi CG, Silini A, Fiorini C, et al., 2005, Mutational Analysis of Human BAFF Receptor TNFRSF13C (BAFF-R) in Patients with Common Variable Immunodeficiency. *J Clin Immunol*, 25(5): 496-502.
- [21] Pham LV, Fu L, Tamayo AT, et al., 2011, Constitutive BR3 Receptor Signaling in Diffuse, Large B-Cell Lymphomas Stabilizes Nuclear Factor-KappaB-Inducing Kinase While Activating Both Canonical and Alternative Nuclear Factor-KappaB Pathways. *Blood*, 117(1): 200-210.
- [22] Parameswaran R, Muschen M, Kim Y-M, et al., 2010, A Functional Receptor for B-Cell-Activating Factor Is Expressed on Human Acute Lymphoblastic Leukemias. *Cancer Res*, 70(11): 4346-4356.
- [23] Kern C, Cornuel J-F, Billard C, et al., 2004, Involvement of BAFF and APRIL in the Resistance to Apoptosis of B-CLL through an Autocrine Pathway. *Blood*, 103(2): 679-688.
- [24] Endo T, Nishio M,ENZLER T, et al., 2007, BAFF and APRIL Support Chronic Lymphocytic Leukemia B-Cell Survival through Activation of the Canonical NF-KappaB Pathway. *Blood*, 109(2): 703-710.
- [25] Suliman BA, Xu D, Williams BRG, 2012, The Promyelocytic Leukemia Zinc Finger Protein: Two Decades of Molecular Oncology. *Frontiers in Oncology*, 2: 74.
- [26] Kolesnichenko M, Vogt PK, 2011, Understanding PLZF: Two Transcriptional Targets, REDD1 and Smooth Muscle A-Actin, Define New Questions in Growth Control, Senescence, Self-Renewal and Tumor Suppression. *Cell Cycle*, 10(5): 771-775.
- [27] Cheung M, Pei J, Pei Y, et al., 2010, The Promyelocytic Leukemia Zinc-Finger Gene, PLZF, Is Frequently Downregulated in Malignant Mesothelioma Cells and Contributes to Cell Survival. *Oncogene*, 29(11): 1633-1640.
- [28] Topalian SL, Hodi FS, Brahmer JR, et al., 2012, Safety, Activity, and Immune Correlates of Anti-PD-1 Antibody in Cancer. *New England Journal of Medicine*, 366(26): 2443-2454.
- [29] Brown SD, Warren RL, Gibb EA, et al., 2014, Neo-Antigens Predicted by Tumor Genome Meta-Analysis Correlate with Increased Patient Survival. *Genome Research*, 24(5): 743-750.
- [30] Zheng X, Song X, Shao Y, et al., 2018, Prognostic Role of Tumor-Infiltrating Lymphocytes in Esophagus Cancer: A Meta-Analysis. *Cell Physiol Biochem*, 45(2): 720-732.

- [31] Tan LY, Martini C, Fridlender ZG, et al., 2017, Control of Immune Cell Entry through the Tumour Vasculature: A Missing Link in Optimising Melanoma Immunotherapy?. *Clinical & Translational Immunology*, 6(3): e134.
- [32] Zingg U, Montani M, Frey DM, et al., 2010, Tumour-Infiltrating Lymphocytes and Survival in Patients with Adenocarcinoma of the Oesophagus. *European Journal of Surgical Oncology*, 36(7): 670-677.
- [33] Schreiber RD, Old LJ, Smyth MJ, Cancer Immunoediting: Integrating Immunity's Roles in Cancer Suppression and Promotion. *Science*, 331(6024): 1565-1570.
- [34] Linsley PS, Chaussabel D, Speake C, 2015, The Relationship of Immune Cell Signatures to Patient Survival Varies Within and Between Tumor Types. *PLoS One*, 10(9): e0138726.
- [35] Chen K, Zhu Z, Zhang N, et al., 2017, Tumor-Infiltrating CD4+ Lymphocytes Predict a Favorable Survival in Patients with Operable Esophageal Squamous Cell Carcinoma. *Medical Science Monitor*, 23: 4619-4632.
- [36] Kavanagh ME, Conroy MJ, Clarke NE, et al., 2016, Impact of the Inflammatory Microenvironment on T-Cell Phenotype in the Progression from Reflux Oesophagitis to Barrett Oesophagus and Oesophageal Adenocarcinoma. *Cancer Lett*, 370(1): 117-124.
- [37] Sarvaria A, Madrigal JA, Saudemont A, 2017, B Cell Regulation in Cancer and Anti-Tumor Immunity. *Cell Mol Immunol*, 14(8): 662-674.

**Publisher's note**

Bio-Byword Scientific Publishing remains neutral with regard to jurisdictional claims in published maps and institutional affiliations.